ORIGINAL PAPER

Zinc sulfide surface formation on Hg electrode during cyclic voltammetric scan: an implication for previous and future research studies on metal sulfide systems

I. Ciglenečki · E. Bura-Nakić · M. Marguš

Abstract Cyclic voltammetry on the Hg electrode was used to investigate the electrochemical behavior of NaCl/NaHCO$_3$ electrolyte solutions supersaturated with respect to Zn sulfide phases. The voltammetric results clearly show how an Hg electrode, due to exchange between Hg^{2+} from an HgS$_{adlayer}$ and Zn^{2+} from solution, becomes the site for surface ZnS$_{adlayer}$ formation in the potential range −0.45 to −0.6 V. The exchange reaction is reversible, and the surface-formed ZnS$_{adlayer}$ persists at the Hg electrode surface until −1.3 V during cathodic scans. Near −1.3 V, it is reduced. In the same solution, evidence for reduction of bulk Zn sulfide species including nanoparticles was not obtained. The approach emphasized here can be readily extended to any other system consisting of metal electrode and chalcogenide anions, pointing to the importance of choosing experimental conditions (i.e., deposition potential, stirring, and accumulation times) to avoid artifacts and wrong interpretation of data due to surface formation of metal sulfide species.

Keywords Metal sulfides electrochemistry · ZnS nanoparticles · Hg electrode · Cyclic voltammetry

Introduction

Electrochemical determination of sulfur species on Hg electrodes is based on the formation of HgS layers at potentials more positive than −0.6 V vs. Ag/AgCl [1]. The anodic electrode reaction is a two-electron reversible process involving oxidation of mercury to mercuric ions with immediate formation of insoluble HgS. Usually, well-separated voltammetric peaks are observed for the anodic deposition of HgS, but only one peak is observed for the cathodic dissolution of HgS [1–4]. The reduction of HgS layers is often used for the quantitative determination of sulfur species in natural waters [3–6].

Recently, adsorptive cathodic stripping voltammetry on Hg electrodes has been proposed as a method for determination of chalcogenide nanoparticles in model solutions and complex natural samples [7–11]. Mercury electrodes preconcentrate metal sulfide nanoparticles effectively, enabling their detection at submicromolar concentrations in cathodic scans that reduce them to amalgams and free sulfide. Mercury electrodes are able to acquire voltammetrically active sulfide nanoparticles by two mechanisms: (a) adsorption to Hg electrodes where they undergo reduction at −0.9 to −1.35 V (vs. Ag/AgCl) in cathodic scans and (b) formation directly at the Hg electrode surface in supersaturated metal sulfide solutions [8, 10]. The second mechanism does not acquire nanoparticles in the solution. In order to avoid HgS electrodeposition as a source of adlayers consisting of secondary sulfides, potentials more negative than −0.85 V (vs. Ag/AgCl) have been proposed for accumulating sorbed Cu$_x$S nanoparticles from the solution [8]. Bura-Nakić et al. [9] tested this approach for Pb^{2+} and Hg^{2+} sulfide solutions and suspensions of HgS and S^0 powders. The resulting reduction peaks were assigned to reduction of nanoparticles from the solution, while the shapes and positions of these peaks were explained as consequence of the chosen experimental conditions (ionic strength, deposition potential, deposition time, ageing of nanoparticles) [9]. In the case of FeS nanoparticles, oxidation of Hg by FeS at around −0.45 V is the operating mechanism for their determination in aqueous solution [11].

In this work, evaluation of experimental conditions as well as metal ion influence on the HgS reduction/disolution

I. Ciglenečki (✉) · E. Bura-Nakić · M. Marguš
Center for Marine and Environmental Research,
Ruđer Bošković Institute,
Bijenička 54,
10000 Zagreb, Croatia
e-mail: irena@irb.hr

process is performed. Problems related to complexity of cathodic stripping electrode processes of sparingly soluble compounds formed at the Hg electrode surface are demonstrated on the example of Zn sulfide/sulfur/polysulfide systems. Voltammetric measurements by employing cyclic voltammetry (CV) and, in some cases, square voltammetry (SWV) were performed in supersaturated solutions regarding to ZnS in order to assess the possibility of electrochemical determination and characterization of ZnS nanoparticles. The results obtained clearly show: (1) that electroreduction of bulk ZnS nanoparticles was not recorded at given experimental conditions and (2) the importance of selected experimental conditions, i.e., deposition potential and deposition (accumulation) time for avoiding artifacts that could give rise to an erroneous interpretation of data due to surface formation of metal sulfide species, i.e., $ZnS_{adlayer}$ during cyclic voltammetric scan.

Experimental part

All chemicals used were of reagent grade and were not further purified. Milli-Q water was used for the preparation of all solutions. The electrochemical measurements were done with BAS-100B electrochemical analyzer (Bioanalytical Systems, West Lafayette, IN, USA) connected to hanging Hg drop electrode as working electrode. As reference electrode, Ag/AgCl (saturated NaCl) was used and a platinum wire served as auxiliary electrode. The electrochemical technique used was cyclic and square wave voltammetry (Cv, SWV). All measurements were done in supporting electrolyte solution containing 0.55 M NaCl/3×10^{-2} M NaHCO$_3$ at a pH range of around 8.5. Deposition of metal sulfide species on Hg surface, depending on concentration range, was done either by stirring the electrolyte solution during deposition step at starting potential and/or without deposition step. Stock solutions of S^{2-} and S$_4^{2-}$ were prepared by dissolving Na$_2$S (Kemika, Croatia) and Na$_2$S$_4$ (Alfa Products), respectively, in a solution of 2×10^{-4} M NaOH which was deoxygenated by bubbling with extra-pure nitrogen. A stock solution of elemental sulfur (S^0) was prepared by dissolving elemental sulfur in toluene. All investigated solutions were prepared by mixing adequate aliquots of Zn^{2+} and either S^{2-}, S^0, and S$_4^{2-}$ stock solutions in deoxygenated supporting electrolyte directly in an electrochemical cell a few minutes before measurement. Precision of measurements (current, potential, and charges) are ±10%.

Results and discussion

### Electrolyte solution containing Zn^{2+} and S^{2-}

It is known that Zn^{2+} reacts with S^{2-} to produce ZnS. In supersaturated solution, ZnS colloids will be formed [12].

Typical CV curves, obtained 5 min after mixing equimolar concentrations of the Zn^{2+} and S^{2-}, are given in Fig. 1, curve 1. Formation of colloidal ZnS was confirmed by light scattering and UV/VIS measurements. After deposition at −0.05 V (t_D= 30 s), a negative going-scan was performed, yielding a C2/A2 peak couple, which represents the well-known dissolution/deposition of HgS$_{adlayer}$ on the Hg electrode surface [1–4]:

$$HS^- + Hg^0 \rightleftarrows HgS_{adlayer} + H^+ + 2e^- \qquad (1)$$
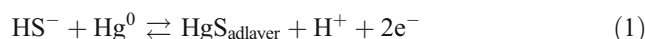
At higher Zn^{2+} concentration, beyond equimolar point, a new C3/A3 peak pair appeared (Fig. 1, curves 2 and 3). On curve 2, both C2 and C3 peaks are visible, while at higher Zn^{2+}/S^{2-} ratio only C3 was detected. Please be aware that changes in background current of curve 2 and 3 are due to
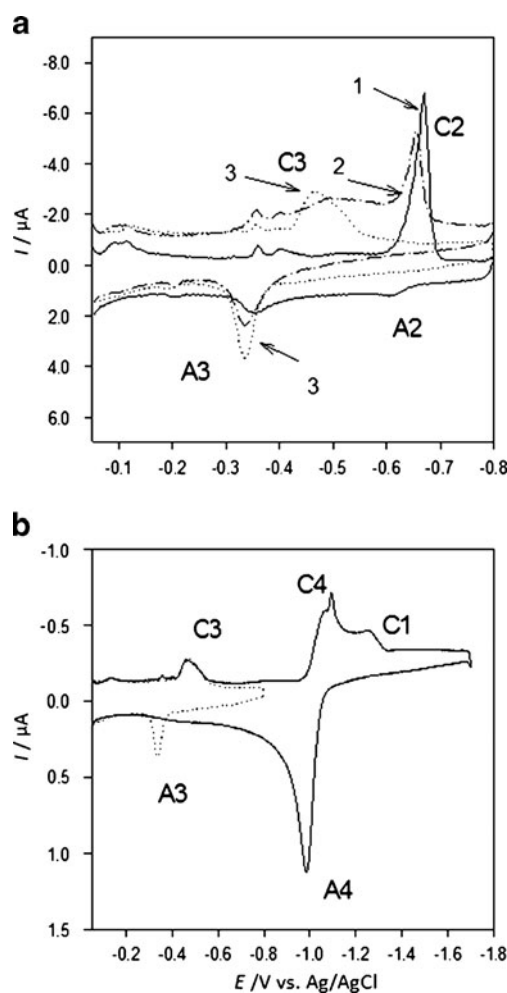

Fig. 1 a CVs for: 3×10^{-5} M Zn^{2+} and 3×10^{-5} M Na$_2$S (*curve 1*); 5×10^{-5} M Zn^{2+} and 3×10^{-5} M Na$_2$S (*curve 2*); 1×10^{-4} M Zn^{2+} and 3×10^{-5} M Na$_2$S (*curve 3*) in 0.55 M NaCl/3×10^{-2} M NaHCO$_3$, pH=8.5–9. Deposition potential, E_D=−0.05 V, initial potential, E_I=−0.05 V, deposition time, t_D=30 s, scan rate, v=0.1 Vs^{-1} and CV switching potential, E_{SP}=−0.8 V. **b** The same as curve 3 from **a** with different CV switching potentials, E_{SP}=−1.7 V (*dashed curve*) and E_{SP}=−0.8 V (*solid curve*)

traces of oxygen which penetrated in the solution during addition of Zn^{2+}.

If the scan was extended to −1.7 V, then C4/A4 and C1 peaks were revealed (Fig. 1b, dashed curve). The C4/A4 peak pair can be assigned to reduction/oxidation of Zn^{2+} at the mercury electrode surface [13]:

$$Zn^0 \rightleftarrows Zn^{2+} + 2e^- \qquad (2)$$

while in accordance with the literature the C3/A3 peak pair can be assigned to the reversible electrochemical exchange reaction with Hg [14–18]:

$$ZnS_{adlayer} + Hg^0 \rightleftarrows HgS_{adlayer} + Zn^{2+} + 2e^- \qquad (3)$$
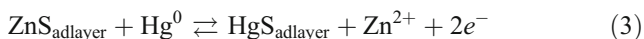
A similar exchange mechanism is observed in electrolyte solutions containing Fe and sulfide species. Furthermore, the same anodic oxidation of Hg by FeS at around −0.45 V is proposed as an analytical protocol for electrochemical determination of FeS nanoparticles in natural waters [11].

According to our study, it appears that the formal potential of the electrode reaction 3 is related to the solubility product of the ZnS since we found that in the case of FeS [11], which is more soluble, and CdS [unpublished data], which is less soluble, in the same experimental conditions this potential is positioned around 150 mV more negative and/or positive, respectively. Such explanation is fully in line with Banica et al. [14] who showed that a similar exchange reaction with Cd^{2+} is occurring at a potential of −0.3 V. Thus, the whole process can be defined as a competition in the formation of two insoluble compounds, i.e., HgS and ZnS in the diffusion layer, considering that the concentration of Hg^{2+} varies with electrode potential. It is important to notice that at the given experimental conditions, above and in all experiments later, the coverage of electrode by HgS layer was under a monolayer coverage (180 μC/cm^2) [1].

The A3 peak was visible only if the CV switching potential (E_{SP}) was more positive than the C1 peak potential (Fig. 1b, dotted curve), and roughly its charge corresponds to the C1 peak charge. The C1 peak increases with accumulation at deposition potentials more positive than −0.5 V in the same proportion as the C3 reduction peak, i.e., charge of the C1 always corresponds to charge of the C3 peak. At the same time, C1 varies linearly with increasing Zn^{2+} concentrations. These facts imply a direct relationship between the C1 peak and the amount of surface-formed $ZnS_{adlayer}$ at the C3 peak potential. Therefore, the C1 peak can be ascribed to the reduction of $ZnS_{adlayer}$ on the Hg surface [19, 20]:

$$ZnS_{adlayer} + 2e^- + H^+ \rightarrow Zn^0 + HS^- \qquad (4)$$
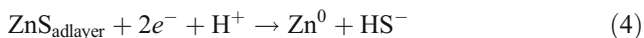
Zn^0 formed at the C1 peak is oxidized at the A4 peak potential according to reaction 2.

The A3 peak is very sensitive to small changes in the deposition potential (E_D) as presented in Fig. 2a. In Fig. 2b,
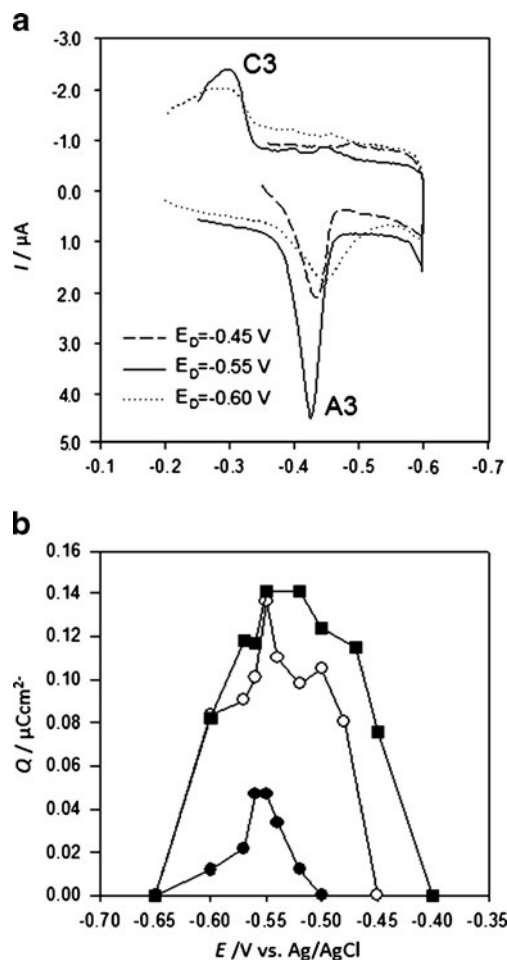
Fig. 2 **a** CV curves at different E_D (see key) for 2×10^{-5} M Zn^{2+}, 3.4×10^{-5} M Na_2S in 0.55 M NaCl/3×10^{-2} M NaHCO$_3$, pH=8.5. $E_I=E_D$, t_D=30 s, v=0.05 Vs^{-1}. **b** Dependence of A3 peak charge on E_D for different concentrations of Zn^{2+}: *filled circles*, 1.1×10^{-5} M; *open circles*, 1.6×10^{-5} M; *filled squares*, 2.8×10^{-5} M; other conditions as in **a**

the charge of A3 peak is given in relation to E_D for different concentrations of S^{2-} and Zn^{2+}. At potentials more positive than −0.40 V, $HgS_{adlayer}$ would be formed preferentially and no A3 peak would be recorded. As E_D becomes more negative than −0.40 V, i.e., between −0.65 and −0.40 V, and reaches the potential of $ZnS_{adlayer}$ (C3) formation, the charge of A3 peak increases and reaches its maximum (Fig. 2b). In given experimental conditions, the charge of A3 is limited by the concentration of S^{2-} in the HgS layer. As E_D becomes more negative than −0.65 V, reaction 3 cannot proceed due to $HgS_{adlayer}$ dissolution from the electrode surface, and consequently an A3 peak is not observed.

It is important to notice that in the same solution reduction and/or oxidation of ZnS nanoparticles from bulk solution is not detected and the obtained HgS reduction peak is only a measure of unreacted, free S^{2-} maintained by ZnS solubility. Contrary to this behavior, CuS and FeS nanoparticles

contribute to HgS formation by the same anodic process as described by reactions 1 and 3 [7, 11].

Why ZnS nanoparticles do not adsorb at the Hg electrode surface can be probably explained by the different surface properties of ZnS nanoparticles than those previously investigated (Cu_xS, PbS, HgS, and FeS). In the literature, it is stated that chemisorption of water at the ZnS nanoparticle surface leads towards a reversible structural modification without change in nanoparticle size [21, 22]. A wide-angle X-ray scattering investigation showed that a more crystalline structure is obtained when water interacts with the nanoparticle [21]. Molecular dynamics (MD) simulations indicate strong water interactions with the surface of ZnS nanoparticles while the enthalpy changes associated with water adsorption were estimated to be ~500 kJ per mol H_2O. This indicates both strong interactions between water and the surface and a very large stabilization effect [21]. The MD simulations predict that the polar water molecules orient to permit hydrogen and oxygen bonding to the terminating S and Zn ions [23, 24]. Strong adsorption of water molecules on the ZnS nanoparticle surface would make them extremely stable and surface S atoms would not be in direct contact with the Hg electrode surface. This most probably disables their adsorption and reduction at the Hg electrode surface. To clarify this possibility, we run several experiments in water–methanol mixtures to see if the resulting change in surface hydration changes the electrochemical behavior of ZnS. Unfortunately, the preliminary test was negative, and no electrochemical signal of ZnS nanoparticles from solution was revealed in pure methanol and methanol–water mixtures.

Electrolyte solutions containing Zn^{2+} and S^0

Evidence that C3/A3 and C1 peaks are produced by a surface reaction mechanism and that they do not arise from analytes in bulk solution, i.e. Zn sulfur complexes or nanoparticles, is proved again by CV scans in mixtures of Zn^{2+} and elemental sulfur (S^0). In these mixtures, when formation of ZnS nanoparticles was not expected and not detected, the same peaks as with sulfide solution were recorded (Fig. 3a). Since the electrochemical behavior of dissolved S^0 at the Hg electrode is the same as that reported for sulfide, at potentials more positive than −0.6 V HgS will be formed [6]. During the negative CV scan, Zn^{2+} from the solution will replace Hg from HgS and at the C3 potential $ZnS_{adlayer}$ will be formed.

In the same solution, we showed that the C3 peak potential is a logarithmic function of the Zn^{2+} concentration (Fig. 3b) with a slope RT/nF of 0.017 V, which is close to the theoretical value expected for a reversible process (0.013 V) [14]. The overall charge of both peaks C2 and C3 was constant and independent on the Zn^{2+} concentration, proving that the amount of S^{2-} at the Hg surface layer
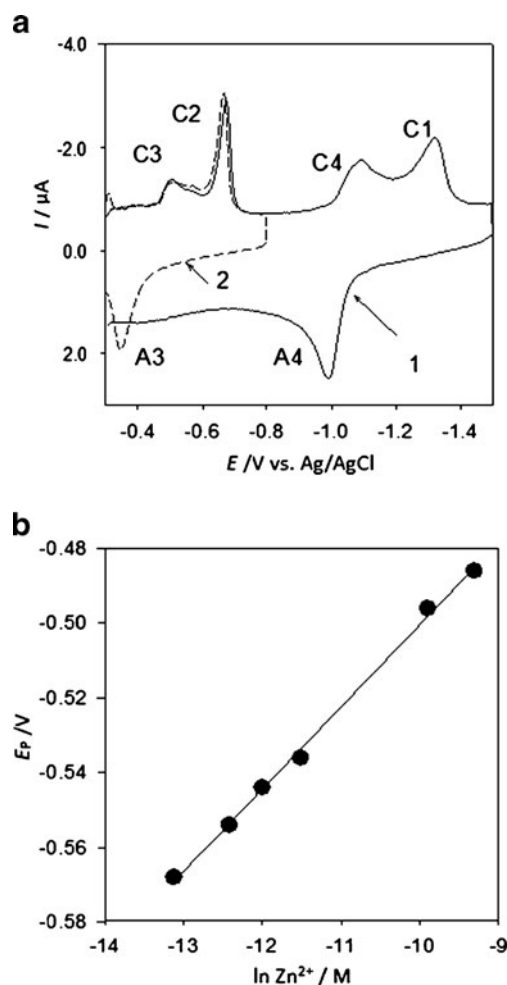

Fig. 3 **a** CV curves for 2×10^{-5} M Zn^{2+} and 8×10^{-6} M S^0 in 0.55 M NaCl/3×10^{-2} M $NaHCO_3$. Deposition potential, $E_D = -0.2$ V, initial potential, $E_I = -0.2$ V, deposition time, $t_D = 30$ s, scan rate, $v = 0.1$ V s^{-1}. **b** Zn^{2+} effect on the cathodic reaction of HgS from **a**. Varied CV switching potential, $E_{SP} =$ var. Other conditions as in **a**

remains constant and that no additional Zn^{2+} and S^{2-} complex formation occurs [14].

The influence of different E_D on C1, C2, and C3 peak charges is shown in Fig. 4. After deposition at potentials ranging from −0.2 to −0.65 V ($t_D = 30$ s), negative-going scans were performed. At these potentials, HgS will be preferably formed which, during negative scan, will be replaced by ZnS. The results showed that the charge of the C1 peak reaches maximum values when the applied E_D was between −0.45 and −0.6 V (Fig. 4a). At these potentials during accumulation, parallel HgS and ZnS will be formed on the electrode surface and depending on the Zn^{2+} concentration, i.e., beyond equimolar point, only C1 peak will be revealed. Figure 4b shows A3 peak charge dependence on the CVs switching potential under conditions where E_D and t_D were held constant prior to the scan in the negative-going direction. When the CV switching potential reaches the C1 peak potential range, the A3 peak disappeared. This result indicates that a $ZnS_{adlayer}$ that formed
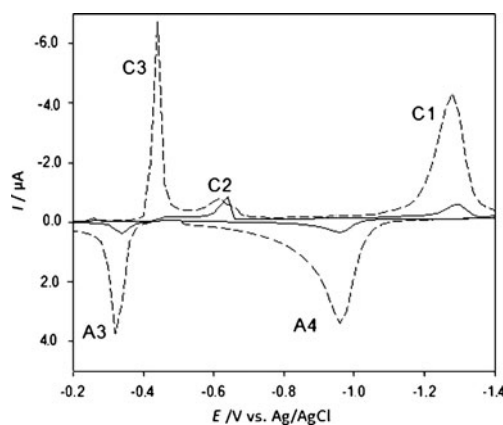
a

b
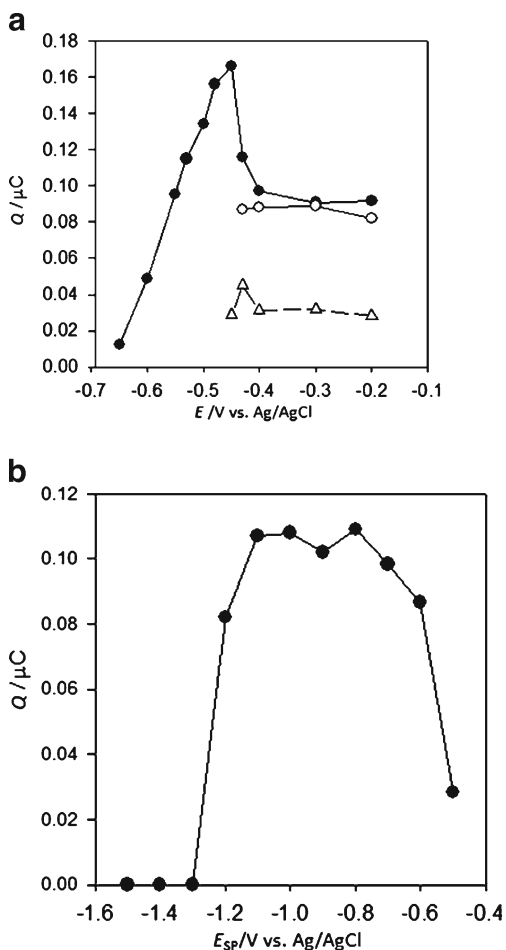
Fig. 4 Solution composition of 2.0×10^{-5} M Zn^{2+} and 8×10^{-6} M S^0 in 0.55 M NaCl/3×10^{-2} M NaHCO$_3$ electrolyte. **a** Dependence of C1 (*filled circle*), C2 (*open circle*), and C3 (*open triangle*) peak charge on deposition potential, E_D; E_{SP}=−0.8 V; t_d=30 s; v=100 mV/s. **b** Dependence of A3 peak charge on CV switching potential, E_{SP}. E_D= −0.2 V; other conditions as in **a**

Fig. 5 CVs for $2.4e^{-5}$ Zn^{2+} and $2.7e^{-6}$ S_4^{2-} in 0.55 M NaCl/3×10^{-2} M NaHCO$_3$, pH=8.5–9. The electrode was held at deposition potential E_D=−0.5 V for deposition time t_D=0 s (*solid line*) and t_D=30 s (*dashed line*); then, the scan was initiated in the positive direction to first switching potential E_{SP1}=−0.1 V and then to second switching potential, E_{SP2}=−1.4 V at a scan rate of v=100 mV/s

at the C3 peak potential stays at the Hg electrode surface until it is reduced at C1 according to reaction 4. A similar behavior was obtained with a surface-formed FeS$_{adlayer}$, for which reduction starts at a potential more negative than −1.4 V [11].

Implication for analyzing natural samples

In the literature, C1–C4 peaks similar to those recorded here were reported for solutions containing mixtures of Zn^{2+} and different polysulfide species [25, 26]. Reduction peaks at around −1.3 V (C1 in our case) were assigned to the reduction of bulk Zn polysulfide complexes [25, 26]. However, in our work and in our experimental conditions, CV and SWV scans (not shown) in mixtures of Zn^{2+} and tetrasulfide solution produce the same results as we previously obtained with sulfide and elemental sulfur, as shown on Fig. 5, where C1 peak is assigned to the reduction of a surface-formed ZnS$_{adlayer}$. In agreement with results plotted in Fig. 4, for Zn

and S^0 system, the charge of the C1 peak in the case of tetrasulfide was related with A3 peak charge and again was with maximum values when applied E_D was between −0.45 and −0.6 V.

The use of deposition steps has often been criticized, i.e., accumulation with stirring during measurements what would create adsorption peaks and not measure solution species as is expected under diffusion control. In Fig. 5, it is clearly shown that measurements with and without deposition step produce the same results as we expected since the difference between accumulation and diffusion is only in the amount of sulfide species that reaches the Hg electrode. With accumulation step at starting potential, usually all of the above recorded peaks were increasing, although their currents were limited either by concentration of S^{2-} or Zn^{2+} in diffusion layer. A similar effect was observed by changing the scan rate and usually C3, C1, and A3 have a linear relation with the scan rate. Evidence in this paper supports the work of Banica et al. [14] who already have emphasized the complexity of the electrochemical reactions involving sulfide anions, Hg, and second metal which have been considered the most in using DeFord–Hume method in the characterization of soluble metal ion complexes with HS$^-$ [27]. These authors used voltammetry at Hg electrode to monitor the sulfide peak in order to determine stability constants for metal sulfide complexes in seawater [27]. Usually, they titrated sulfide with metals and monitored the decrease and shift of the HgS reduction peak, which starts to broaden when the total metal concentration exceeds the sulfide concentration. The same effect was recorded by polysulfide and thio-compounds [25, 26, 28]. By a similar approach, the distribution of sulfide was monitored in natural waters, where distinction was made between free and complexed sulfide, depending on the position of the recorded peak

potentials [29]. Considering the results described here with Zn sulfur systems or the results recently published for Fe [11], it is likely that serious errors might arise when analyzing natural samples as well as model systems when the above-mentioned peaks, recorded in similar experimental conditions as shown above, are regarded as arising from soluble bulk species.

We know that the Zn^{2+} concentrations used in our experiments are rather high and usually cannot be found in natural waters, but the sulfide and polysulfide concentration are reasonable for anoxic environment [30, 31] where they can produce similar adlayers at the Hg electrode in combination with a sufficiently high concentration of Fe for example and might be a source of potential error.

Conclusion

In this paper, it is clearly shown how surface $ZnS_{adlayer}$ formation at the Hg electrode is possible by the exchange reaction of mercury from HgS with Zn^{2+} from the solution. The exchange reaction is reversible and well-defined reduction/oxidation peaks were observed at −0.5 and −0.38 V, respectively. Surface-formed $ZnS_{adlayer}$ stays at the Hg electrode surface until reduction at around −1.3 V. At the same time, reduction of bulk ZnS species including nanoparticles is not observed, implying that ZnS nanoparticles do not behave in the same way as previously investigated in CuS, PbS, HgS, and FeS nanoparticles. This work clearly shows how metal sulfide deposits can form directly on the electrode surface if the solution composition and the electrochemical accumulation conditions are appropriate. These deposits and their corresponding reduction peaks do not necessarily reflect the bulk situation.

References

1. Krznarić D, Ciglenečki I (2005) Electroanalysis 17:1317–1324
2. Redinha JS, Politeiro C, Pereira JLC (1997) Anal Chim Acta 351:115–120
3. Krznarić D, Ciglenečki I, Ćosović B (2001) Anal Chim Acta 431:269–278
4. Luther GW, Giblin AE, Varsolona R (1985) Limnol Oceanogr 30:727–736
5. Bura-Nakić E, Viollier E, Jezequel D, Ciglenečki I (2009) Chem Geol 266:320–326
6. Ciglenečki I, Ćosović B (1997) Electroanalysis 9:1–7
7. Ciglenečki I, Krznarić D, Helz GR (2005) Environ Sci Technol 39:7492–7498
8. Krznarić D, Helz GR, Ciglenečki I (2006) J Electroanal Chem 59:207–214
9. Bura-Nakić E, Krznarić D, Jurašin D, Helz GR, Ciglenečki I (2007) Anal Chim Acta 594:44–51
10. Krznarić D, Helz GR, Bura-Nakić E, Jurašin D (2008) Anal Chem 80:742–749
11. Bura-Nakić E, Krznarić D, Helz GR, Ciglenečki I (2011) Electroanalysis 23(6):1376–1382
12. Daskalakis KD, Helz GR (1993) Geochim Cosmochim Acta 57:4923–4931
13. Van den Berg C.M.G. (1988) Electroanalytical chemistry of seawater. In: Riley JP, Skirow G (eds) Chemical oceanography, vol. 9. Academic, London, pp. 198–245.
14. Banica FG, Galik M, Švancara I, Vytras K (2009) Electroanalysis 21:332–341
15. Winkler K, Kalinowski S, Krogulec T (1988) J Electroanal Chem 252:303–322
16. Winkler K, Krogulec T (1995) J Electroanal Chem 386:127–134
17. Winkler K, Krogulec T (1985) Electrochim Acta 30:1055–1062
18. Itabashi E (1981) J Electroanal Chem 117:295–307
19. Valiuliene G, Žieliene A, Jasulaitiene V (2003) Chemija 14:128–134
20. Pilyte S, Valiuliene G, Žieliene A, Vinkevičius J (1997) J Electroanal Chem 436:127–132
21. Zhang H, Gilbert B, Huang F, Banfield JF (2003) Nature 424:1025–1029
22. Goseami N, Sen P (2004) Solid State Commun 132:791–794
23. Zhang H, Rustad JR, Banfield JF (2007) J Phys Chem A 111:5008–5014
24. Goodell C, Gilbert B, Weigand S, Banfield JF (2008) J Phys Chem C 112:4791–4796
25. Chadwell SJ, Rickard D, Luther GW (2001) Electroanalysis 13:21–29
26. Chadwell SJ, Rickard D, Luther GW (1999) Aquat Geochem 5:29–57
27. Luther GW III, Rickard D, Theberge SM, Olroyd A (1996) Environ Sci Technol 30:671–679
28. Luther GW III, Theberge SM, Rickard D (2000) Talanta 51:11–20
29. Luther GW III, Church TM, Powell D (1991) Deep Sea Res 38(2):s1121–s1137
30. Bura-Nakić E, Helz GR, Ciglenečki I, Ćosović B (2009) Geochim Cosmochim Acta 73:3738–3751
31. Helz GR, Bura-Nakić E, Mikac N, Ciglenečki I (2011) Chem Geol 284:323–333